Journal of Rehabilitation in Civil Engineering 13-4 (2025) 190-206

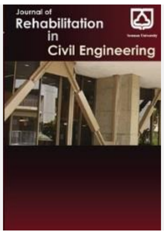

Journal of Rehabilitation in Civil Engineering

Journal homepage: https://civiljournal.semnan.ac.ir/

Structural Analysis of Two Flexible Pavements Subjected to Groundwater Table Rising Considering Unsaturated Behaviour of Subgrade Soil

Mohammed Bouatia [1, 2 *]

1. LGC-ROI, Laboratoire de Génie Civil-Risques et Ouvrages en Interaction, Department of Civil Engineering, University of Batna 2-Mustafa Ben Boulaid, 0578 Batna, Algeria
2. LTPiTE, Laboratoire Travaux Publics, ingénierie des Transports Environnement, Ecole Nationale Supérieure des Travaux Publics, 16051 Algiers, Algeria

*Corresponding author: *m.bouatia@univ-batna2.dz*

ARTICLE INFO

Article history:
Received: 29 July 2024
Revised: 01 December 2024
Accepted: 15 January 2025

Keywords:
Flexible pavement;
Subgrade;
Service duration;
Resilient modulus;
Unsaturated soil.

ABSTRACT

In flexible pavements, the resilient modulus (RM) of the subgrade layer is crucial for ensuring the serviceability of these structures throughout their lifespan. This research presents a 3D numerical analysis of the two most commonly used flexible pavement structures in the Algerian road network, GB/GB and GB/NTG, considering the effect of subgrade RM vulnerability to groundwater table (GWT) fluctuations. The first pavement structure is Gravel-Bitumen/Gravel-Bitumen (GB/GB), and the second is Gravel-Bitumen/Non-Treated-Gravel (GB/NTG), denoting the materials composing the base and subbase layers, respectively. To investigate pavement-subgrade interaction, four GWT levels (120m, 60m, 30m, and 15m) were used to assess the structural performance of the analyzed flexible pavements taking into account the effect of the unsaturated behavior of the subgrade soil subjected to GWT rises from 120m to 15m depth. Based on the conditions outlined in the Algerian Manual for New Pavement Design (AMNPD), the numerical simulations were conducted using the advanced FLAC3D software. The results of computed von Mises stresses and induced deflections indicated that the loss of suction, due to GWT rise, can impose substantial additional loads on pavement structures. Further analysis using Alize-LCPC software revealed that a Groundwater Table rise from 120m to 15m could reduce the service duration by over 11 years for GB/GB and over 14 years for GB/NTG pavement structures. Moreover, regression models were developed to predict deflection and von Mises stresses with reliable accuracy ($R^2 > 0.90$). Regardless cost considerations, the study concludes that the GB/NTG pavement structure outperforms the GB/GB pavement structure in terms of durability and performance considering similar scenarios.

E-ISSN: 2345-4423

How to cite this article:
Bouatia, M. Structural Analysis of Two Flexible Pavements Subjected to Groundwater Table Rising Considering Unsaturated Behaviour of Subgrade Soil. Journal of Rehabilitation in Civil Engineering, (2025), 190-206. https://doi.org/10.22075/jrce.2025.34801.2146

1. Introduction

Highways are linear infrastructures designed to provide optimal support for vehicles. Pavements, as a fundamental structural element of such lifelines, play a crucial role in ensuring the functionality and durability of these transportation networks. Pavements are substantial budgetary projects, designed to endure for a 20-year service duration [1]. Therefore, they necessitate maintenance and protective measures to ensure long-term performance and durability, as annual pavement damages result in significant costs to the transportation systems [2]. Flexible pavements generally comprise asphalt concrete laid atop granular base and subbase layers, which are supported by a compacted soil layer known as the subgrade [3,4]. Environmental factors such as precipitation, temperature, freeze-thaw cycles significantly affect the performance of flexible pavements. Additionally, groundwater table depth influences the extent of environmental impacts on pavement structural performance [5,6]. As a multilayer system, the performance of a pavement structure is significantly influenced by the stiffness of each layer [7]. The Resilient Modulus (RM) is used in pavement engineering to characterize road unbound granular materials and subgrade soils to design pavement structures [8–10], in both empirical and mechanistic empirical methods [11]. El-Hamrawy and Abd El-Hakim [12] reported that the fatigue lifespan of pavements improves with higher subgrade stiffness. However, changes in moisture content within the subgrade layer of flexible pavement can significantly impact its structural performance by affecting the overall stiffness of the pavement system as concluded by Elshaer et al [13]. Consequently, this accelerates pavement deterioration and shortens its lifespan by promoting the softening of subgrade materials [14]. As porous mediums, the mechanical properties of pavement subgrades are significantly influenced by the behavior of partially saturated soil. Standard compaction specifications mandate the compaction of subgrade layer soils in the field at or close to optimal water content and at a specified percentage of the maximum dry unit weight. Therefore, subgrade soils are in an unsaturated state during the construction stage as well as along the service duration [15], endowing them with stiffer behavior attributed to additional interparticle normal forces from suction [16]. Many researchers have reported the sensitivity of unsaturated subgrade soils to moisture content [17–19]. Considering cohesive soils, Zhang et al. [20] observed that the resilient modulus (RM) is proportional to the matric suction. Through a parametric study carried out using a back-propagation artificial neural network on 124 CPT data profiles, Ghanizadeh et al. [11] reliably confirmed the inverse relation between the resilient modulus of clayey subgrade soils and moisture content. These findings were confirmed by Ji & al [8] for all types of soils. Unfortunately, in many scenarios, subgrade soils undergo moisture variations due to environmental events such as rainfall infiltration or fluctuation of the GWT that follows sea level rise or inundation, which leads to a significant reduction in RM due to saturation [21]. Elshaer and Daniel [22] reported that inundation, leading to saturated conditions, has a significant impact on the structural performance of flexible pavements. Their analysis revealed that saturation causes a 15 to 80% increase in vertical strain at the top of the subgrade layer. Chen and Wang [23] demonstrated that sea level rise significantly affects pavement performance, particularly during seasons with higher GWT. Their findings revealed that under the impact of GWT rise, the compressive strain on the subgrade increases more noticeably than the tensile strain at the bottom of the asphalt layer. Knott et al. [24] investigated the effect of GWT rising due to sea level rise on five coastal roads in New Hampshire, USA. They found that all the analyzed roads experienced a reduction in the service duration.Economically, Ali [25] reported that the cost increase resulting from a reduction in design life and higher maintenance expenses can reach up to 84%, depending on the type of subgrade soil and the elevation of the groundwater table (GWT).

Based on the literature review, limited research has investigated the structural performance and quantified the reduction in pavement service duration due to environmental factors affecting subgrade performance. The significant economic and environmental impacts of damage to highway infrastructures underscore the importance of considering the unsaturated behavior of subgrade soils in road design and construction. Ensuring road safety and durability requires comprehensive design studies that account for material properties (subgrade and pavement layers) and environmental factors (GWT fluctuation, rainfall, temperature). This approach is essential for predicting and mitigating potential damage to pavement structures, typically constructed on unsaturated platforms within the vadose zone.

This research is part of a research project on road safety and performance under environmental influences. Specifically, the paper examines the structural behavior of flexible pavements in areas with fluctuating GWT. Using the powerful FLAC^{3D} code, a 3D numerical analysis is conducted to evaluate the structural behavior of two flexible pavements subjected to GWT rise as an environmental factor which reduces the RM of the subgrade layer due to saturation. Two of the most used flexible pavement structures, in Algeria, were selected to conduct the simulations. In the AMNPD, the minimum subgrade RM value defined to design subgrade layers of national roads pavements is 50 MPa, which is equivalent to a platform class S2 or PF50. These simulations aimed to study the performance and service duration susceptibility of pavements when subjected to a reduction in the initially designed resilient modulus (RM) of subgrade soil, which occurs due to loss of suction that follows GWT rising. The analyzed pavement structures are GB/GB and GB/NTG abbreviations that reflect the materials that constitute the base and subbase layers, respectively. The GB refers to Gravel/Bitumen which is a Hot Mixed Asphalt (HMA) material while the NTG abbreviates Non-Treated Gravel material. Using widely accepted models to simulate the mechanical behavior of subgrade unsaturated soil, four GWT levels were considered: GWT=120m, 60m, 30m, and 15m to investigate the GWT rising influence on the subgrade-pavement interaction. Consequently, four platform classes PF(gwt=120m), PF(gwt=60m), PF(gwt=30m), and PF(gwt=15m) are resulted in. Using the calculated platform classes, the analysis is focused on the investigation of the effect of the GWT rising on the two flexible pavements considering: (1) Deflection magnitudes which represent downward displacement and (2) von Mises stresses (VMS) computed within the pavement layers in response to traffic loads. Reliable regression models ($R^2 > 0.90$) to predict the deflection amplifications that reached 150% were proposed. Besides, the impact of groundwater table (GWT) rise on the service duration of both pavement structures was quantified. It was found that the service duration can be shortened by up to 86% for GB/GB and 68% for GB/NTG pavement structures. Furthermore, comparisons between the obtained results from both structures were provided and commented to help engineers and practitioners making better and more effective decisions in similar scenarios.

2. Methodology

In the last decades, the FEM computational technique was efficiently utilized within the domain of road engineering [26]. A 3D numerical simulation is conducted to analyze the structural response of two flexible pavements under a scenario involving subgrade resilient modulus (RM) reduction that may follow environmental triggering factors such as rainfall infiltration or groundwater table fluctuations. Considering the unsaturated behavior of subgrade soils in pavement engineering, this research focuses on the assessment of the GWT rising as an environmental factor to assist practitioners (i.e., engineers) in predicting one of the likely causes of numerous damages recorded along road infrastructures that results in disruption of traffic flows and service duration reduction. The flowchart provided in Fig. 1 outlines the main steps to perform the present analysis.

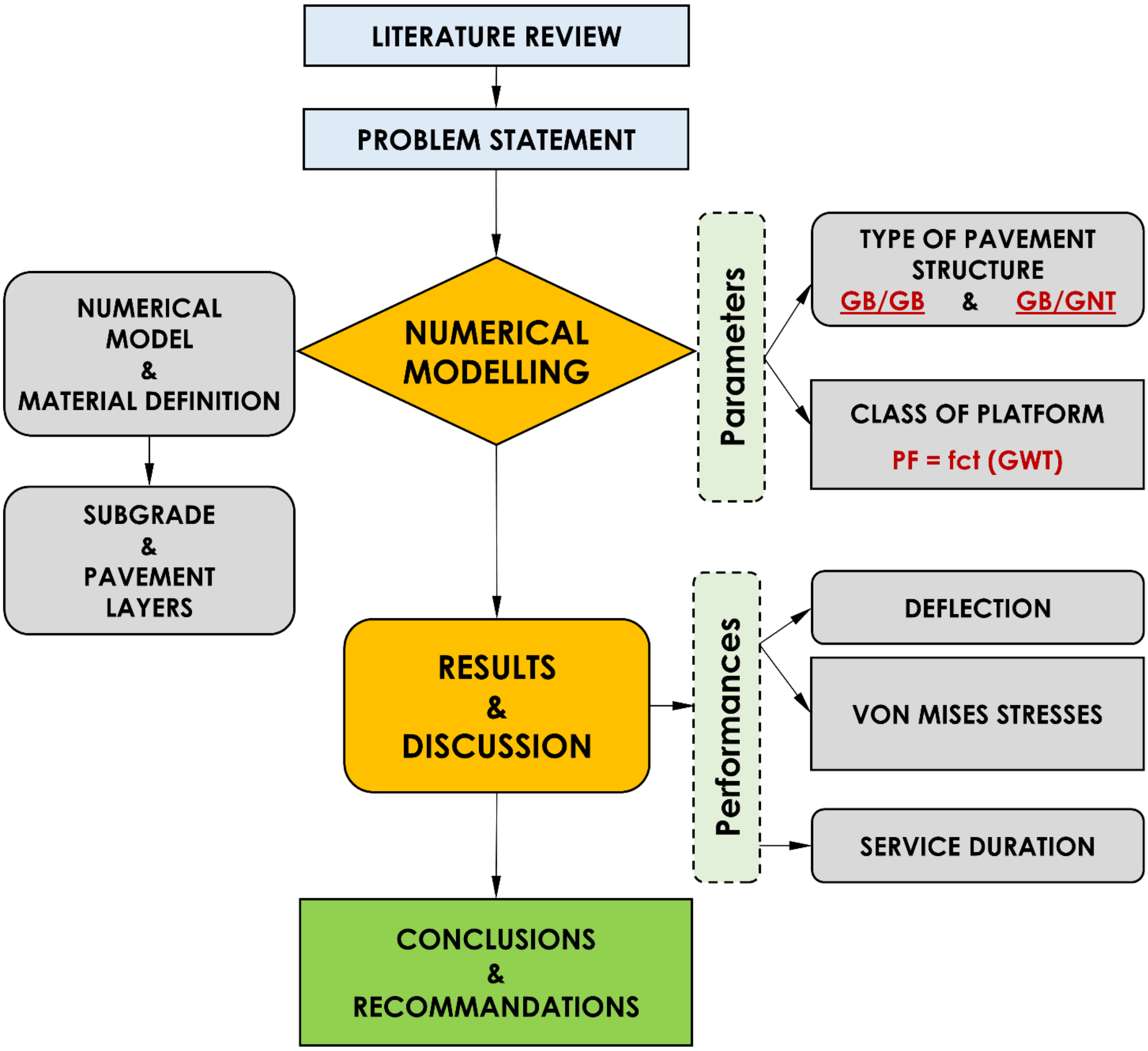

Fig. 1. Flowchart of the present study.

3. Numerical model

The present research is a 3D numerical analysis of the subgrade-pavement interaction considering the unsaturated behavior of subgrade soils of flexible pavements under the effect of GWT rising. Based on the project importance, traffic flow, loading conditions, and materials availability, the AMNPD proposes numerous pavement structures with various combinations of materials type and thicknesses to ensure the structural performance of the Algerian road network. As the GB/GB and GB/NTG are the most used flexible pavement structures to build national roads in Algeria, the simulations were performed using these two pavement structures. For both pavement structures, the numerical model is composed of three layers that constitutes the pavement structure which overly the foundational subgrade layer. A quarter symmetry is employed to simulate the structural response of the pavement under traffic loading using the powerful code FLAC^{3D} [27]. The quarter symmetry was adopted to reduce the time required for calculation and to keep the realistic three dimension of the problem. The geometry of the numerical model was constructed by assembling eight node brick primitives (Fig. 2). To avoid the boundary condition influence in lateral and bottom directions, the radius of the model as well as the thickness of the subgrade layer are set equals to 2000 mm. In FLAC^{3D} software, the ratio of the maximum unbalanced force to the gravitational body force acting on the nodes of the numerical model is defined as the convergence criterion to determine if the simulation has reached equilibrium. The default value of this ratio is adopted in the present study (i.e., 10^{-5}). The simulation of the mechanical behavior of the subgrade soil is detailed in the coming sections.

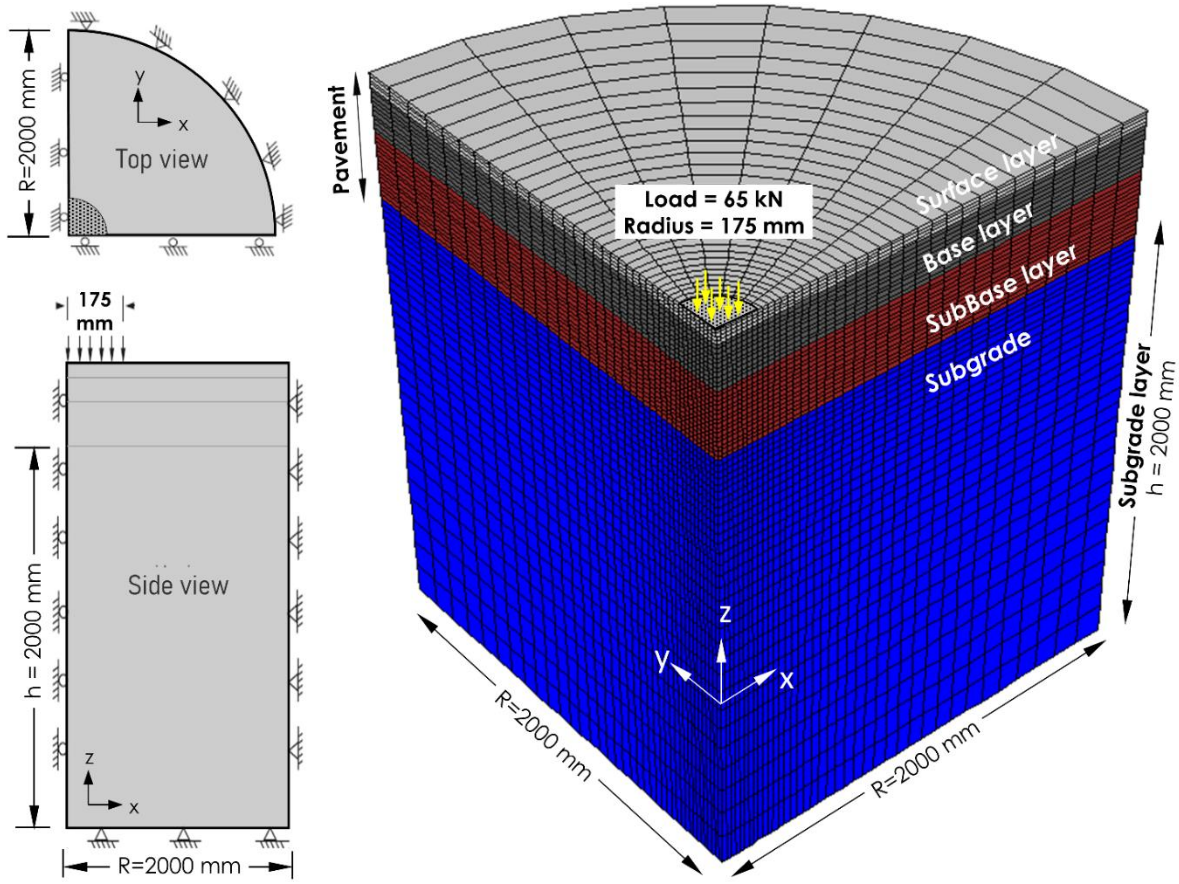

Fig. 2. Numerical model and details of boundary conditions.

The used boundary conditions are depicted in the left side of the Fig. 2 (see Top view and side view). The displacements at the symmetry boundaries (x = 0 and y = 0) are restricted along the x- and y-axes, respectively. In addition, the movements of both lateral circumferential and bottom nodes are constrained in x, y and z-directions. The pavement structures were meshed as detailed in Table 1 where Zone I represents the areas under the wheel loading (Radius≤175mm). The bracketed letters (R) and (P) reflect Regular and Progressive size variation of the brick primitives that constitute the concerned layer.

Table 1. Vertical and horizontal meshing (Numbers of brick primitives).

	Vertical		Horizontal	
Layer	GB/GB	GB/GNT	Zone I (Radius≤175mm)	Zone II (R>175mm)
Surface	4 (R)	4 (R)	8 (R)	20 (P)
Base	6 (R)	10 (R)	8 (R)	20 (P)
SubBase	6 (R)	15 (R)	8 (R)	20 (P)
Subgrade	30 (P)	30 (P)	8 (R)	20 (P)

The applied load on the pavement can be simulated using either point loads or circular loads with uniform pressure [4]. The AMNPD detailed the loading conditions as follow: the wheel load is simulated as a vertical downward uniform stress equals to 0.675 MPa applied on the contact gridpoints wheel/pavement. The latter is assumed to be a circle of 350 mm diameter to transfer a load of 65 kN [28,29]. The acceleration due to gravity is set to 9.81 m/s². The interface between the layers of a pavement plays a crucial role in its behavior and structural performance. In this simulation, the interface between two adjacent layers of the pavement structure consider no relative displacements between the contact gridpoints where the surficial nodes are totally attached. The simulations were performed in three main steps: (1) creating the geometry of the numerical model, (2) calculating the initial stress state (i.e., geostatic stresses), and (3) applying a uniform circular load stress on the TSP to simulate the loading conditions.

4. Materials

In the realm of pavement engineering, multiple methodologies are employed to design pavements, often using the application of fundamental linear elastic theory [30–32]. This approach assumes an elastic, isotropic, and homogeneous nature of all materials involved [31,33]. This paper utilizes the linear elastic constitutive model to simulate the behavior of the pavement multilayer system. Typically, the essential parameters for each layer consist of the elastic modulus (E), Poisson's ratio (ν), and the thickness (h) of the layer.

4.1. Soil of the subgrade layer

By adopting the Young's modulus of the subgrade soil, the AMNPD groups the Algerian lands into five platform classes S0, S1, S2, S3, and S4. However, S3 and S4 are not accepted classes and should be improved to achieve the minimum allowed value of RM (at least 50 MPa) that corresponds to a CBR value not lesser than 10. In the literature, numerous studies have documented that the modulus of elasticity of partially saturated soils increases as soil suction rises [16]. Subgrades, being unsaturated soils, are prone to changes in humidity where saturation that follow a rising of the GWT results in a decrease in the RM [15] which will affects the structural performance of such structures. Considering the unsaturated behavior of subgrade soils, this research aims to assess the structural response of two flexible pavements subjected to the rising of GWT level by analyzing the effect of suction variations on the RM. The soil used to perform this research is taken from Aine-Tine municipality (Mila province, Algeria). It constitutes the subgrade that support the pavement of the national highway RN79. The users of this road are daily suffering due to its low serviceability caused by repetitive deformations caused by the damages that affected the subgrade layer. The national highway RN79 relates Mila province with the southern and eastern provinces of the country (i.e., Batna, Constantine, Setif). To perform the analysis, four GWT depths were considered as follow: 120m, 60m, 30m, and 15m. The initial GWT depth is set at 120m which will be raised to be firstly: 60m, secondly: 30m and finally: 15m. As a result, the computed suction values of the subgrade layer decrease due to saturation. The calculated profiles P1, P2, P3, and P4 of suction distribution along the depth of the 2m thick subgrade layer are presented in Fig 3. These profiles were computed using the linear simplified model that relates the suction values to the depth from the GWT level, using gravity (g=9.81 m/s²) (see right side in Fig. 3).

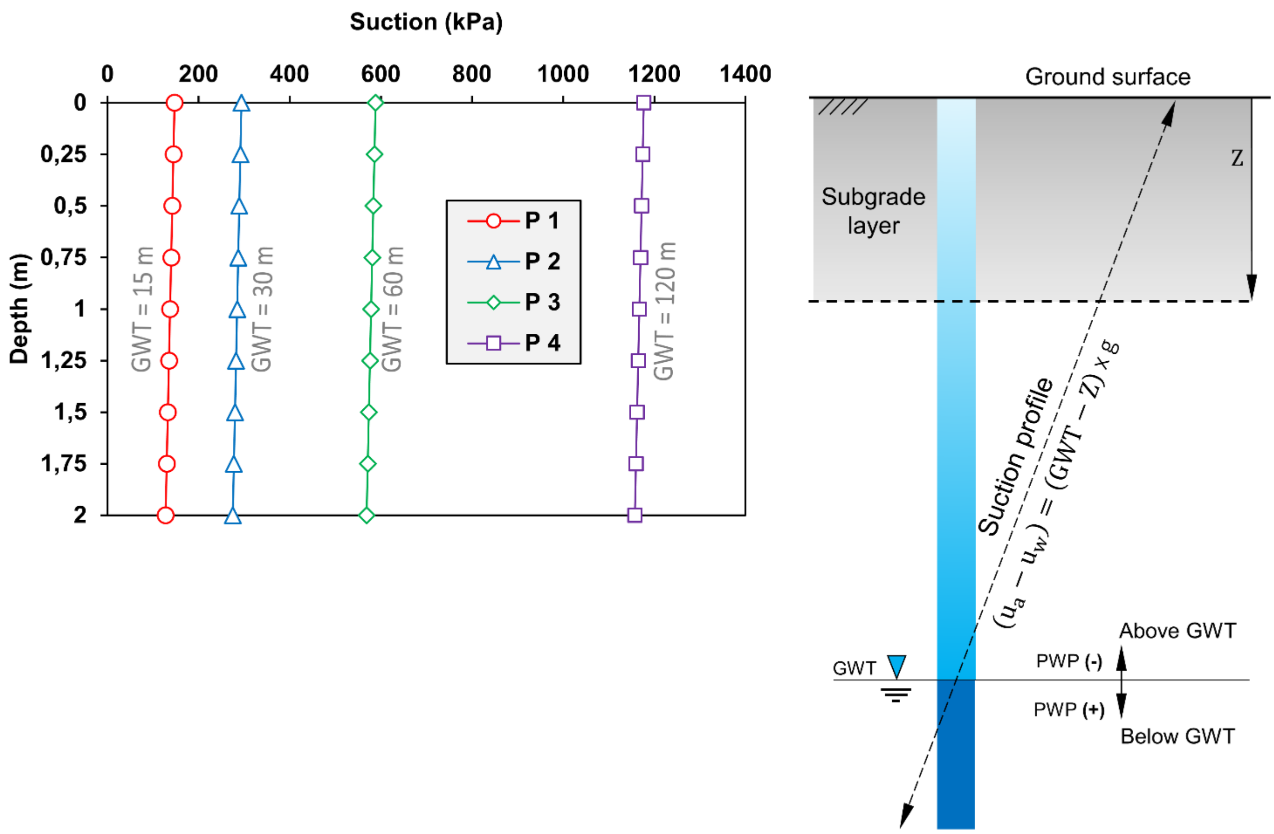

Fig. 3. Suction variation profiles considering different GWT levels.

The calculation of the unsaturated young's modulus E_{unsat} of the subgrade soil is performed using the model proposed by Oh et al. [34] (Equation. 1). This model is widely accepted and used in the field of unsaturated soils for its simplicity and effectiveness to simulate the behavior of such soils.

$$E_{unsat} = E_{sat}\left[1 + \alpha\,\frac{(u_a - u_w)}{(P_a/101.3)}(S)^{\beta}\right] \tag{1}$$

Where; E_{unsat} is the unsaturated young's modulus; E_{sat} = 1000 kPa is the young's modulus in saturated conditions; P_a is the atmospheric pressure (100 kPa); $(u_a - u_w)$ is the suction within the soil; S is the degree of saturation; α=0.1 and β=2 are fitting parameters that allows to use this equation in the case of Aine-Tine soil [35]. The degree of saturation calculation is performed using the widely used model proposed by van Genuchten [36] presented in equation 2.

$$S = S_r + \frac{1 - S_r}{\left[1 + \left(\frac{u_a - u_w}{a}\right)^n\right]^m} \tag{2}$$

Where S is the degree of saturation, S_r is the residual degree of saturation and a, n, and m are fitting parameters where $n = 1/(1-m)$. These parameters equal to 0.5 kPa, 1.08 and 0.07, respectively. More details about the Aine-Tine soil investigation can be found in Bouatia [35]. Fig. 4 presents the results of the unsaturated young's modulus profiles E-P4, E-P3, E-P2 and E-P1 calculated throughout the depth of the 2m thick subgrade layer for GWT depths: 120, 60, 30 and 15m, respectively. To simplify the simulations, the subgrade RM is assumed to remain constant throughout the subgrade layer's depth (i.e., h=2000 mm) by considering a mean value of the unsaturated young's modulus for each GWT depth. Consequently, the adopted RM values are as follow: 58, 31, 17 and 9 MPa that corresponds to GWT rising from 120m, 60m, 30m to 15m, respectively (see Fig. 4). In the coming sections of this research, the obtained subgrade RMs are denoted platform classes as follow: PF58, PF31, PF17 and PF9.

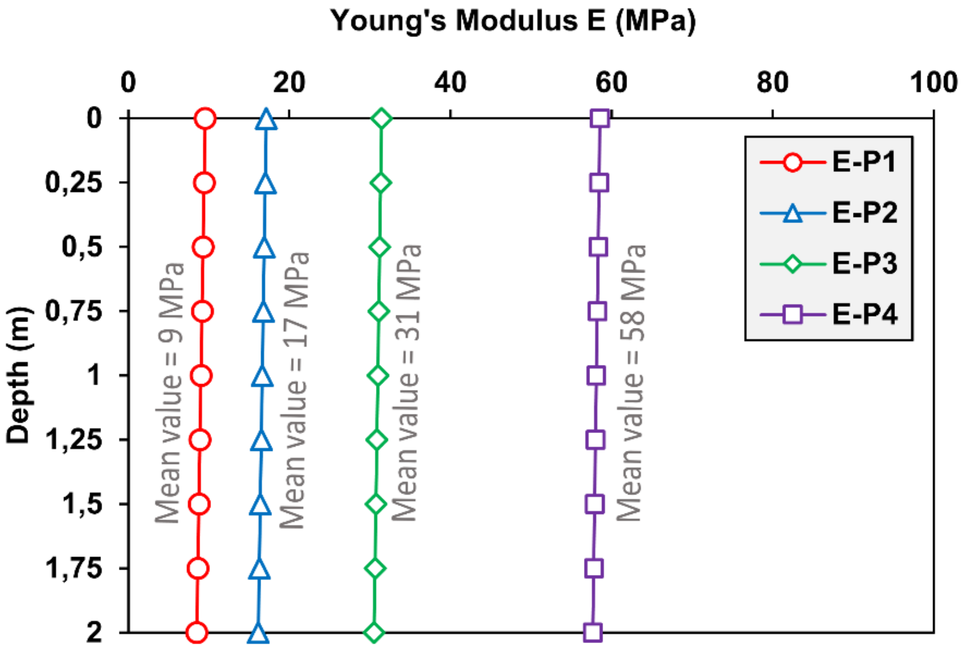

Fig. 4. RM variation profiles along the depth with respect to GWT level.

4.2. Flexible pavement layers

In Algeria, the most commonly used pavement structures for building national roads are flexible structures. This study adopted two flexible pavement structures named GB/GB and GB/NTG In accordance with the naming convention of the AMNPD, the GB/GB and GB/NTG denote the materials used in the Base and Subbase layers, respectively. For 20 years' service duration and a traffic flow growth rate of 4% [37], they are designed to support a daily traffic flow ranging from 600 to 1500 HGV (i.e., Heavy Good Vehicle). Both structures include a surface layer measuring 60 mm thick, consisting of bituminous concrete (HMA with particle size grading of 0/14). In both pavements, the base layer consists of Gravel-Bitumen material (HMA of particle size grading of 0/20) with 110 mm and 200 mm thick for the GB/GB and GB/NTG structures, respectively. The difference between the two pavement structures lies in the subbase layer. The GB/NTG pavement structure includes a 300 mm thick Non-Treated Gravel subbase layer, whereas the GB/GB pavement structure features a 120 mm thick of Gravel-Bitumen. The cumulative thickness of the GB/GB pavement structure equals to 290 mm, while that of the GB/NTG pavement structure measures 560 mm. As bituminous materials are viscoelastic, their Young's modulus changes with temperature. Given Algeria's vast geographical expanse, the AMNPD suggests three equivalent temperatures (i.e., T= 20 °C, T= 25 °C, and T= 30 °C) to account for the viscoelastic behavior of bituminous materials across the entire country. In this study, an equivalent temperature of 30 °C is chosen to consider the most challenging conditions that result in lower Young's modulus values of the bituminous materials. Table 2 summarizes the materials characteristics adopted in this study.

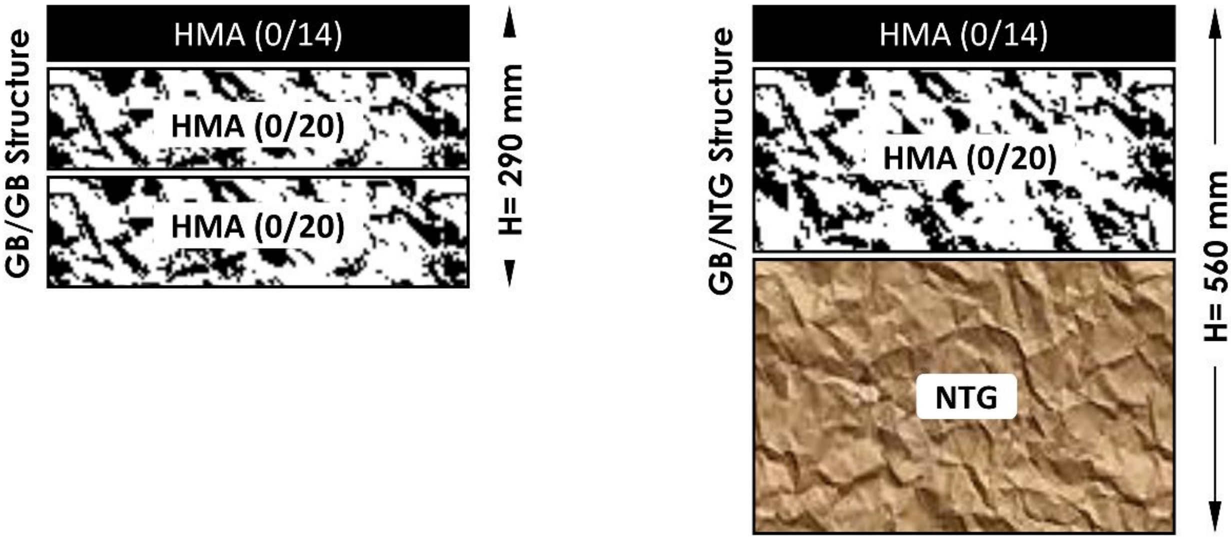

Fig. 5. Details of the two used pavement structures [38].

Table 2. Pavement materials mechanical characteristics.

	Moduli of Elasticity E (MPa)	Poisson ratio ν	Density (kg/m3)
HMA (0/14)	2500 (T=30 °C)	0.4	2400
HMA (0/20)	3500 (T=30 °C)	0.4	2300
NTG (Unbound)	350	0.3	2300
Subgrade (Soil)	PF58 (GWT=120m) = 58 PF31 (GWT=60m) = 31 PF17 (GWT=30m) = 17 PF9 (GWT=15m) = 9	0.4	2200

5. Results and discussion

The study examines the structural response of two flexible pavements, taking into account the impact of rising GWT on the mechanical behavior of the subgrade. It includes discussion about (1) the computed deflections at the TSS and at the TSP in addition to (2) the von Mises stresses computed within the pavement layers. Finally, the effect of the GWT rising on the service duration of the analyzed pavements is evaluated.

5.1. Deflecions

Deflection is widely used criterion to decide reliable design and rehabilitation operations of flexible pavements. It represents the vertical displacement computed at the top surface of the pavement. Fig. 6 depicts the computed deflection contours with respect to GWT depth for both pavement structures (Radius =1m). The presented plots are provided for comparison where for both pavement structures, decreasingly, the deflection magnitudes propagate radially and in-depth starting from the wheel-pavement contact surface. Besides, it was found that the stiffer the subgrade layer the lower the computed magnitude of deflections. Moreover, for the same platform class, the GB/GB pavement structure exhibited higher deflection magnitudes.

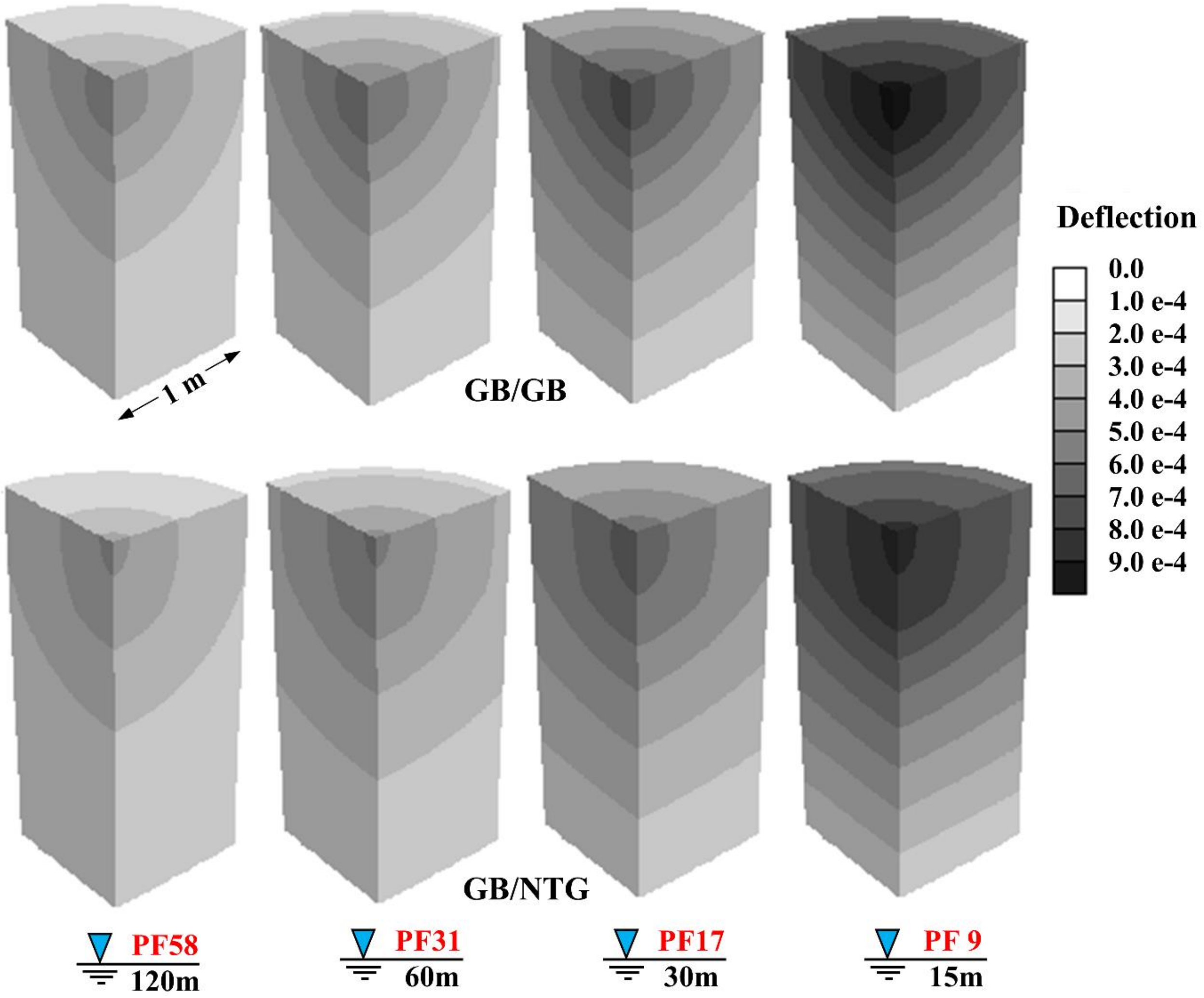

Fig. 6. Deflection distribution for GB/GB and GB/NTG pavement structures (Unit: m).

Fig. 7 - 8 display the deflection values computed at the Top Surfaces of the subgrade and pavement of the GB/GB and GB/NTG pavement structures, respectively. At both locations, an increase in deflection values is observed with respect to the decrease of the platform's RM that follow the GWT rising. This confirms the inverse relationship between the platform's RM and the computed deflections. For the pavement structure GB/GB and the platform class PF58, when the pavement is subjected to a stress of 0.675 MPa, the TSP deflects by 360 µm, whereas a value of 335 µm is computed at the TSS. The computed deflections increased by the subsequent percentages: 35%, 83% and 166% for the TSS, and 32%, 77% and 155% for the TSP, considering the platform classes PF31, PF17, and PF9, respectively. In contrast, for PF58, the GB/NTG pavement structure deflects by 314 at the TSP and by 234 µm for the TSS. For shallower levels of the GWT: 60m, 30m and 15m, the computed deflections increased, respectively, by the following ratios: 42%, 102%, and 218% for the TSP and by: 30%, 75%, and 161% for the TSS. Furthermore, due to the difference in flexural rigidity, one can notice that the GB/GB pavement structure experienced higher deflection magnitudes. The GB/GB and GB/NTG pavement structures have flexural rigidities equal to 3.42 x 10^{13} MPa.mm^4 and 2.40 x 10^{14} MPa.mm^4, respectively.

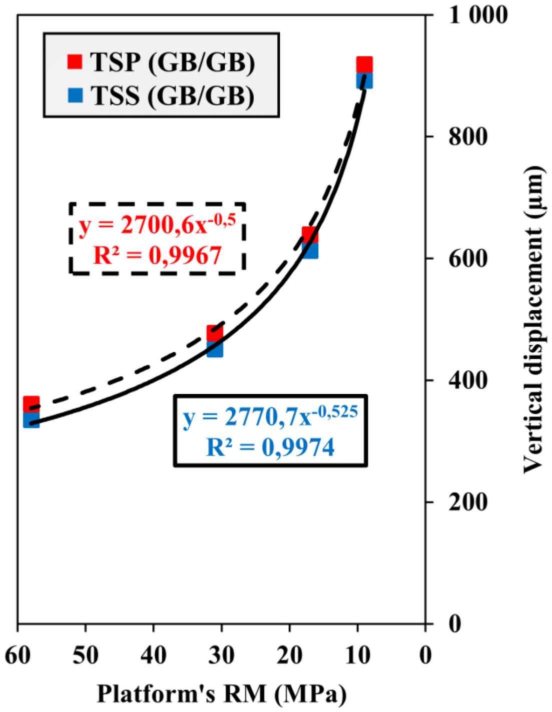

Fig. 7. Computed deflection at the TSS and TSP for PF58, PF31, PF17 and PF9 : GB/GB pavement structure.

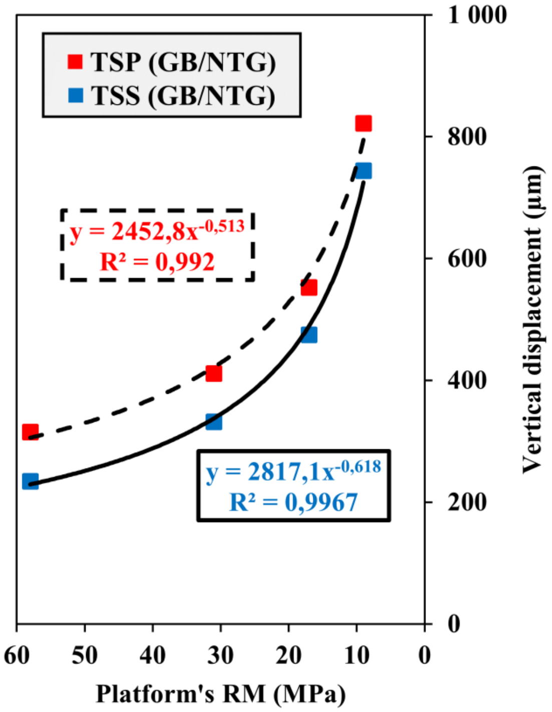

Fig. 8. Computed deflection at the TSS and TSP for PF58, PF31, PF17 and PF9: GB/NTG pavement structure.

From the comparison of the deflections computed at TSS and TSP locations, it was found that the magnitude difference is more pronounced in the GB/NTG pavement structure. This disparity is attributed to the lower RM of the NTG material of the subbase layer that lies beneath the HMA base layer in the GB/NTG pavement structure (i.e., 350 MPa). For both pavement structures, regression models were established to predict the deflection values with respect to the RM of the subgrade layer. The deflection magnitudes were estimated with determination coefficient (R^2) reached 0.99. Using these regression models, it is possible to reliably predict deflection values with respect to the resilient modulus (RM) of the subgrade layer.

5.2. von Mises stress

One of the most used criterion to analyze the structural performance of structures in finite element analysis is the von Mises stress. An embedded programming language in FLAC^{3D} software named FISH that allows users to create new variables and functions to enhance simulation capabilities by incorporating user-defined features. Users can plot or print new variables, implement specialized grid generators, and automate parameter studies [27]. For this reason, a FISH function was used to compute and plot the von Mises stresses for each zone of the numerical model. Consequently, valuable insights to locate and evaluate the critical locations within the pavement structures are provided. Considering the different platform classes, Fig. 9 displays the contours of VMS values computed within both pavement structures. The highest values are concentrated around the loading area. It can be seen that there is an inverse relationship between the computed VMS magnitudes and the platform's RM where higher VMS stresses are observed for lower platform's RM. Regardless of the platform's RM (i.e., PF58, PF31, PF17 and PF9), the GB/GB structure exhibits higher VMS values than those observed in the GB/NTG structure. Furthermore, for both pavement structures, the highest magnitudes of VMSs are concentrated at the bottom of the lowest HMA (Hot Mix Asphalt) layer, specifically at 206 mm and 290 mm from the TSP of GB/NTG and GB/GB structures, respectively. Based on the latter observation, the data of maximum VMS for the Fig. 10 are collected.

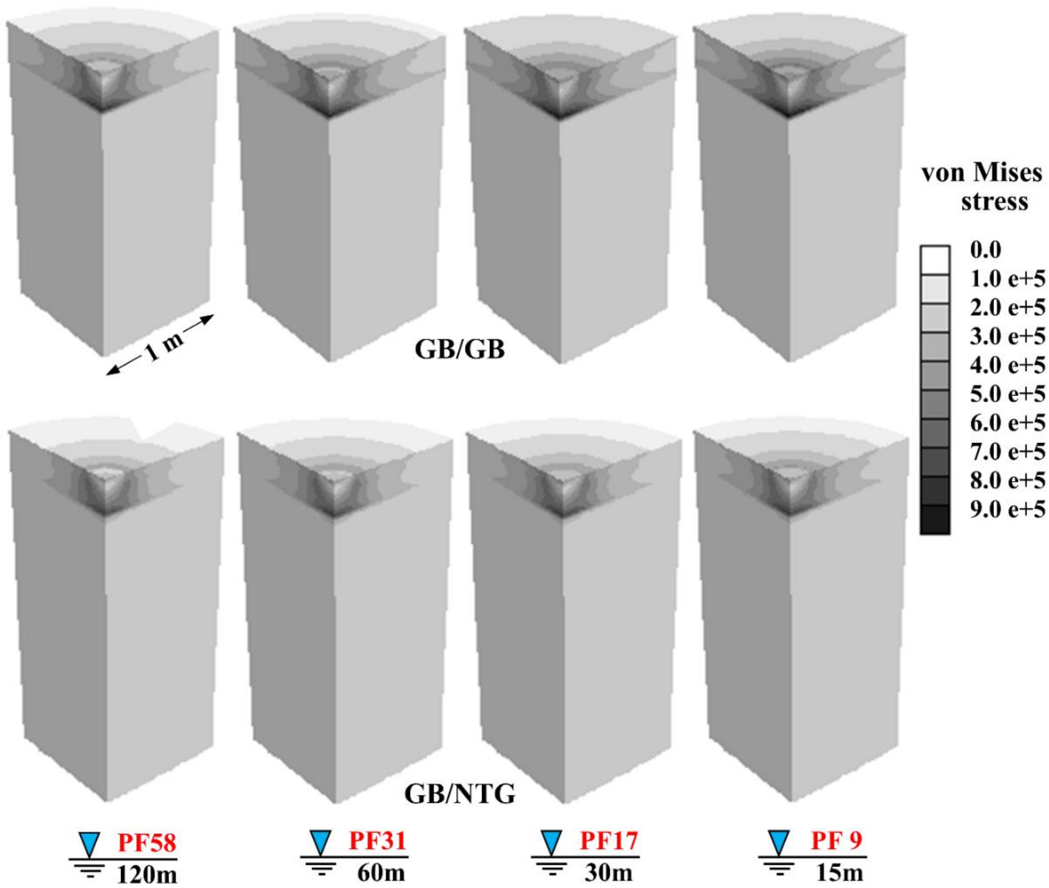

Fig. 9. Contours of von Mises stresses for GB/GB and GB/NTG pavement structures considering platform classes: PF58, PF31, PF17 and PF9 (Unit: Pa).

Fig. 10 illustrates the highest VMS magnitudes computed within the numerical model of both GB/GB and GB/NTG pavement structures. As for the deflection magnitudes, the obtained results highlighted the inverse proportionality between the GWT depth and the computed VMS where the deeper the GWT the lower the VMS values. For the GB/NTG pavement structure, the maximum VMS value for the PF58 platform class that's corresponds to a GWT 120m amounts to 0.560 MPa. However, following the GWT level rising from 120m to 60m, 30m and 15m, this value increased by 22%, 24%, and 26% which corresponds to PF31, PF17, and PF9 platform classes, respectively. Correspondingly, for the same platforms (i.e., PF31, PF17, and PF9), the VMS increases by 8%, 14%, and 18%, respectively, in the GB/GB pavement structure. In contrast, the maximum computed VMS for the PF58 platform class is 0.786 MPa. Linear regression model relating VMSs to the RM of the subgrade layer was established for both pavement structures (see Fig. 10). The determination coefficient (R^2) of the model developed for the GB/GB pavement structure equals to 0.9868 (i.e., Dashed line). Similarly, the R^2 value for the regression model established for the GB/NTG pavement structure reached 0.9229 (i.e., Continued line). These results demonstrate the model's remarkable ability to reliably predict the maximum VMS magnitudes using the RM of the subgrade layer. Consequently, the maximum VMS values can be calculated with a high confidence using the obtained models for subgrade layer RMs ranging between 58 and 9 MPa.

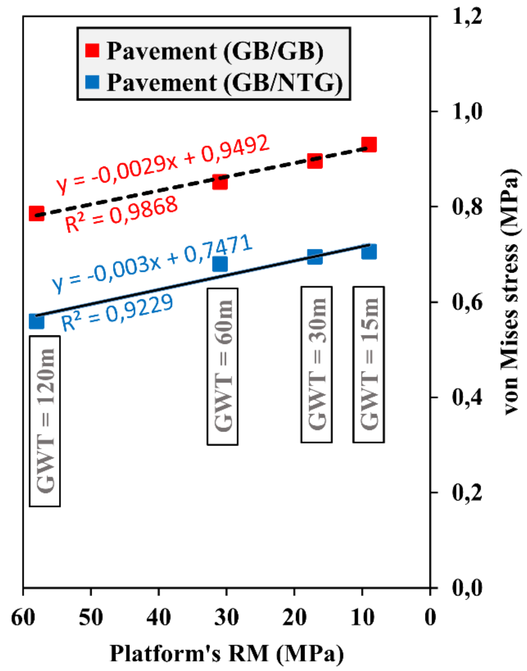

Fig. 10. Maximum von Mises stresses variation for PF58, PF31, PF17 and PF9 (MPa).

5.3. Service duration

Road infrastructures are designed to ensure their functionality and durability throughout their intended service duration, optimizing government investments in transport networks. In the present study, the service duration was back calculated using the back calculation module of Alizé-LCPC software to evaluate the effect of GWT rise on the service duration. This software utilizes a multilayer model [39] that considers isotropic and elastic behavior for the pavement's materials. In addition to design conditions such as traffic, materials, and platform class, the service duration back calculation requires information on allowable horizontal and vertical deformations computed in specific locations within the pavement structure computed considering the new platform class conditions. The AMNPD adopts these deformation criteria to verify the design as well as to back calculate the service duration of flexible pavements. The allowable horizontal deformation $\varepsilon_{t,all}$ is calculated at the bottom of the lowest HMA layer while the allowable vertical deformation $\varepsilon_{z,all}$ is calculated at the TSS. To consider the effect of the GWT rising from 120m, 60m, 30m to 15m, the allowable deformations (i.e., $\varepsilon_{z,all}$, $\varepsilon_{t,all}$) were calculated using the design module of Alizé-LCPC software taking into account the decreased values of subgrade RM (i.e., PF58, PF31, PF17 and PF9). Consequently, two periods of service duration need to be calculated for one pavement structure. The first service duration $N(\varepsilon_{z,all})$ is calculated based on the allowable vertical deformation $\varepsilon_{z,all}$ whereas, the second $N(\varepsilon_{t,all})$ is computed considering the horizontal allowable deformation $\varepsilon_{t,all}$. Subsequently, the service duration of a pavement structure is defined as the minimum of the two obtained service duration $N(\varepsilon_{z,all})$ and $N(\varepsilon_{t,all})$.

Fig. 11 shows the results of the computed service durations with respect to the subgrade's RM for both pavement structures. It was found that the allowable horizontal deformation $\varepsilon_{t,all}$ is the crucial deformation for both structures as it provides the minimum values of service duration whatever the platform class used in this research. For the GB/GB pavement structure (see bleu columns), the service duration is 13.47 years considering the PF58 that corresponds to a GWT depth of 120m. This duration is reduced by 50.7% (i.e., 6.83 years) for the PF31. The reduction ratio reached 74.1% (i.e., 9.99 years) for the PF17 that corresponds to a GWT=30m while it becomes 86.3% (i.e., 11.63 years) for the PF9, resulting in a service duration of 1.84 years which corresponds to a GWT depth of 15m. On the other hand, the computed service durations for the GB/NTG pavement structure are displayed in red columns. For a GWT of 120m depth that results in a subgrade RM of 58 MPa, the initial service duration is 21.7 years. The latter is decreased by 30.2 % (i.e., 6.55 years) for PF31 that corresponds to a GWT rising from 120m to 60m. In the case of 30m GWT depth, the RM becomes 17 MPa and the service duration diminished to 10.4 years which corresponds to a reduction ratio of 52.1% (i.e., 11.3 years). At the last stage of GWT rising (i.e., GWT=15m) when using a platform class PF9, the service duration reduced to 6.9 years. In conclusion, the reduction in RM that follows the rising of the GWT level has a diminishing effect on the service duration of both flexible pavement structures. In addition, the GB/NTG structure outperforming the GB/GB structure, as evidenced by longer computed service durations.

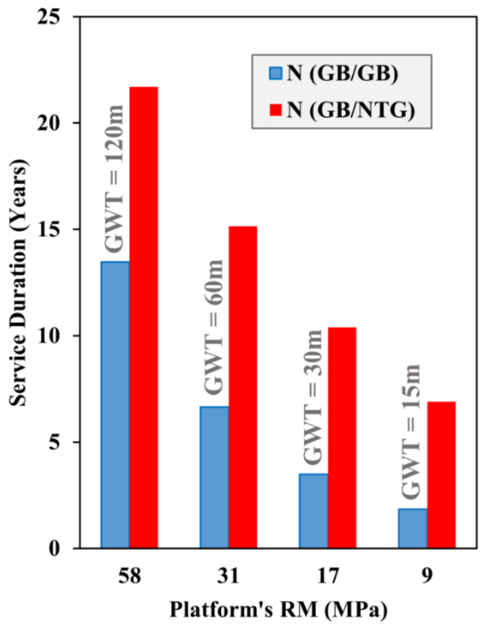

Fig. 11. Service duration variation for the GB/GB and GB/NTG structure with respect to the RM of the platform.

6. Conclusion

This research is part of a project on road safety and performance under environmental influences, specifically examining the structural behavior of flexible pavements in areas with fluctuating GWT. Using the advanced FLAC^{3D} software, we evaluated two flexible pavements through 3D numerical simulation to analyze the effect of GWT rise on the structural response of such structures considering the susceptibility of the subgrade resilient modulus (RM) to moisture content variations. Two of the most used pavement structure types in Algeria, GB/GB and GB/NTG, were selected from the AMNPD to carry out the study. Four GWT levels were considered: 120m, 60m, 30m, and 15m, to investigate the GWT rising effect on the structural performance of flexible pavement. Widely accepted models for partially unsaturated soils were used to consider the unsaturated behavior of subgrade unsaturated soils. The analysis focused on the discussion of the induced deflection magnitudes (vertical displacement) and computed von Mises stresses within the pavement layers under traffic loading. High-determination coefficient regression models ($R^2 > 0.90$) were proposed to predict deflections and von Mises stresses within the two analyzed pavements. Moreover, the impact of GWT rise on the service duration of both pavement structures was quantified and discussed using the ALIZE-LCPC software. Comparisons between the results from both structures were provided to assist engineers and practitioners in making informed decisions. The following conclusions can be drawn:

1. Rising GWT levels from 120m to 15m can drastically reduce the service duration of flexible pavements, potentially shortening it by up to 86% for GB/GB and 68% for GB/NTG pavement structures. These findings can be helpful to explain numerous observed damages in flexible pavements, resulting in significant reductions in their operational lifespan.

2. Increased subgrade saturation amplifies deflections at the pavement surface due to decreased subgrade stiffness following the loss of suction. The GWT rise from 120m to 15m amplifies deflection values by up to 150% for both pavement structures, emphasizing the critical role of subgrade RM in maintaining pavement integrity.

3. The GB/GB pavement structure experienced more significant deformations compared to the GB/NTG configuration due to differences in flexural rigidity. The GB/NTG structure demonstrates a higher service duration under similar subgrade conditions, despite cost considerations.

4. Regression models with high determination factor ($R^2 > 0.90$) were developed to predict deflections and maximum von Mises stresses within both flexible pavements, providing valuable tools for anticipating pavement performance under varying GWT conditions.

In conclusion, the study confirms that the GB/NTG pavement structure offers superior performance compared to the GB/GB structure, providing better resilience against GWT fluctuations and associated subgrade saturation effects. This research underscores the necessity of incorporating the unsaturated behavior of partially saturated subgrades in pavement design to enhance service duration and structural integrity.

Funding

This research is part of a research project on road safety and performance under environmental influences funded by the Algerian ministry of higher education and scientific research. Project ID: PRFU–A01L02UN050220230001

Conflicts of interest

The authors declare that they have no known competing financial interests or personal relationships that could have appeared to influence the work reported in this paper.

Authors contribution statement

Mohammed Bouatia: Conceptualization; Investigation; Methodology; Writing – original draft; Writing.

References

[1] Serin S, Oguzhanoglu MA, Kayadelen C. Comparative analysis of stress distributions and displacements in rigid and flexible pavements via finite element method. Rev La Constr 2021;20:321–31. doi:10.7764/RDLC.20.2.321.

[2] Motamedi M, Shafabakhsh G, Azadi M. Rehabilitation of asphalt binder to improve rutting, fatigue and thermal cracking behavior using nano-silica and synthesized polyurethane. J Rehabil Civ Eng 2021;9:19–28. doi:10.22075/jrce.2019.17579.1335.

[3] Huang YH. Pavement analysis and design. 2nd ed. Pearson Prentice Hall Upper Saddle River, NJ; 2004.

[4] Papagiannakis A, Masad E. Pavement design and materials. Second edi. Hoboken, New Jersey: Wiley; 2024.

[5] Saevarsdottir T, Erlingsson S. Water impact on the behaviour of flexible pavement structures in an accelerated test. Road Mater Pavement Des 2013;14:256–77. doi:10.1080/14680629.2013.779308.

[6] Knott JF, Daniel JS, Jacobs JM, Kirshen P. Adaptation Planning to Mitigate Coastal-Road Pavement Damage from Groundwater Rise Caused by Sea-Level Rise. Transp Res Rec J Transp Res Board 2018;2672:11–22. doi:10.1177/0361198118757441.

[7] Toan TD, Long NH, Wong YD, Nguyen T. Effects of variability in thickness and elastic modulus on the reliability of flexible pavement structural performance. Int J Pavement Eng 2023;24. doi:10.1080/10298436.2022.2039923.

[8] Ji R, Siddiki N, Nantung T, Kim D. Evaluation of resilient modulus of subgrade and base materials in indiana and its implementation in MEPDG. Sci World J 2014;2014. doi:10.1155/2014/372838.

[9] Tiliouine B, Sandjak K. Influence of nonlinear resilient models of unbound aggregates on analysis and performance of road pavements. Period Polytech Civ Eng 2015;59:77–84. doi:10.3311/PPci.7092.

[10] Amakye SYO, Abbey SJ, Booth CA. DMRB Flexible Road Pavement Design Using Re-Engineered Expansive Road Subgrade Materials with Varying Plasticity Index. Geotechnics 2022;2:395–411. doi:10.3390/geotechnics2020018.

[11] Ghanizadeh AR, Ziaie A, Khatami SMH, Fakharian P. Predicting Resilient Modulus of Clayey Subgrade Soils by Means of Cone Penetration Test Results and Back-Propagation Artificial Neural Network. J Rehabil Civ Eng 2022;10:146–62. doi:10.22075/JRCE.2022.25013.1568.

[12] El-Hamrawy S, Abd El-Hakim R. Influence of Subgrade Stiffness on Flexible Pavement Responses – A Case Study-Alexandria City, Egypt. Bull Fac Eng Mansoura Univ 2020;40:49–56. doi:10.21608/bfemu.2020.96398.

[13] Elshaer M, Ghayoomi M, Daniel JS. Methodology to evaluate performance of pavement structure using soil moisture profile. Road Mater Pavement Des 2018;19:952–71. doi:10.1080/14680629.2017.1283356.

[14] Farahani HZ, Farahani A. Study on Drainage of Pavement Layers and Improvement Strategies: Case Study. J Rehabil Civ Eng 2023;11:111–26. doi:10.22075/JRCE.2022.25393.1575.

[15] Sawangsuriya A, Edil TB, Bosscher PJ. Modulus-suction-moisture relationship for compacted soils. Can Geotech J 2008;45:973–83. doi:10.1139/T08-033.

[16] Han Z, Vanapalli SK, Kutlu ZN. Modeling Behavior of Friction Pile in Compacted Glacial Till. Int J Geomech 2016;16. doi:10.1061/(asce)gm.1943-5622.0000659.

[17] Zhang J, Peng J, Zeng L, Li J, Li F. Rapid estimation of resilient modulus of subgrade soils using performance-related soil properties. Int J Pavement Eng 2021;22:732–9. doi:10.1080/10298436.2019.1643022.

[18] Rahardjo H, Melinda F, Leong EC, Rezaur RB. Stiffness of a compacted residual soil. Eng Geol 2011;120:60–7. doi:10.1016/j.enggeo.2011.04.006.

[19] Asadi M, Mallick R, Nazarian S. Numerical modeling of post-flood water flow in pavement structures. Transp Geotech 2021;27:100468. doi:10.1016/j.trgeo.2020.100468.

[20] Zhang J, Peng J, Li J, Zheng J. Variation of Resilient Modulus with Soil Suction for Cohesive Soils in South China. Int J Civ Eng 2018;16:1655–67. doi:10.1007/s40999-018-0315-y.

[21] Luo Q, Ye X, Li Q, Zhang S, Yu Q, Ma X. Experimental and Numerical Study on Response Characteristics of Airport Pavement Subjected to Wetting in Silt Subgrade. KSCE J Civ Eng 2023;27:551–66. doi:10.1007/s12205-022-0647-7.

[22] Elshaer M, Daniel JS. Impact of pavement layer properties on the structural performance of inundated flexible pavements. Transp Geotech 2018;16:11–20. doi:10.1016/j.trgeo.2018.06.002.

[23] Chen X, Wang H. Impact of sea level rise on asphalt pavement responses considering seasonal groundwater and moisture gradient in subgrade. Transp Geotech 2023;40:100992. doi:10.1016/j.trgeo.2023.100992.

[24] Knott JF, Elshaer M, Daniel JS, Jacobs JM, Kirshen P. Assessing the effects of rising groundwater from sea level rise on the service life of pavements in coastal road infrastructure. Transp Res Rec 2017;2639:1–10. doi:10.3141/2639-01.

[25] ALI AM. Influences of water table elevation on structural performance of flexible pavement matrix with different subgrade soil types. 47th IRES Int. Conf., St. Petersburg, Russia: 2016, p. 27–31.

[26] Peng Y, He Y. Structural characteristics of cement-stabilized soil bases with 3D finite element method. Front Archit Civ Eng China 2009;3:428–34. doi:10.1007/s11709-009-0059-5.

[27] ITASCA. FLAC3D Fast Lagrangian Analysis of Continua in 3 Dimensions—User's Guide 2005.

[28] Sandjak K, Tiliouine B. 3D Numerical Investigation of Asphalt Pavements Behaviour Using Infinite Elements. Int J Civ Environ Eng 2018;12:765–72.

[29] CTTP. Catalogue de Dimensionnement des Chaussées Neuves—Fascicule I : Notice d'utilisation 2001.

[30] Papagiannakis AT, Masad EA. Pavement Design and Materials. 2012. doi:10.1002/9780470259924.

[31] Mulungye RM, Owende PMO, Mellon K. Finite element modelling of flexible pavements on soft soil subgrades. Mater Des 2007;28. doi:10.1016/j.matdes.2005.12.006.

[32] Losa M, Natale A Di. Strains in asphalt pavements under circular and rectangular footprints. Balt J Road Bridg Eng 2014;9:101–7. doi:10.3846/bjrbe.2014.13.

[33] Kleizienė R, Vaitkus A, Čygas D. Asfaldi viskoelastsete omaduste mõju katendi käitumisele. Balt J Road Bridg Eng 2016;11:313–23. doi:10.3846/bjrbe.2016.36.

[34] Oh WT, Vanapalli SK, Puppala AJ. Semi-empirical model for the prediction of modulus of elasticity for unsaturated soils 2009;914:903–14. doi:10.1139/T09-030.

[35] Bouatia M. Numerical Analysis of Pipeline Behavior on High Unstable Unsaturated Slope. Case of AEP pipe of Ain Tinn-Mila. University of Mostefa Ben Boulaid - Batna 2, 2021.

[36] van Genuchten MT. A Closed-form Equation for Predicting the Hydraulic Conductivity of Unsaturated Soils. Soil Sci Soc Am J 1980;44:892–8. doi:10.2136/sssaj1980.03615995004400050002x.

[37] CTTP. Catalogue de Dimensionnement des Chaussées Neuves—Fascicule II : Hypothèses et données de dimensionnement 2001.

[38] CTTP. Catalogue de Dimensionnement des Chaussées Neuves—Fascicule III : Fiches techniques de dimensionnement 2001.

[39] Burmister DM. The general theory of stresses and displacements in layered soil systems. II. J Appl Phys 1945;16:126–7. doi:10.1063/1.1707562.